LETTERS

Rapid subtropical North Atlantic salinity oscillations across Dansgaard–Oeschger cycles

Matthew W. Schmidt[1]†, Maryline J. Vautravers[2]† & Howard J. Spero[1]

Geochemical and sedimentological evidence suggest that the rapid climate warming oscillations of the last ice age, the Dansgaard–Oeschger cycles[1], were coupled to fluctuations in North Atlantic meridional overturning circulation through its regulation of poleward heat flux[2]. The balance between cold meltwater from the north and warm, salty subtropical gyre waters from the south influenced the strength and location of North Atlantic overturning circulation during this period of highly variable climate[3–5]. Here we investigate how rapid reorganizations of the ocean–atmosphere system across these cycles are linked to salinity changes in the subtropical North Atlantic gyre. We combine Mg/Ca palaeothermometry and oxygen isotope ratio measurements on planktonic foraminifera across four Dansgaard–Oeschger cycles (spanning 45.9–59.2 kyr ago) to generate a seawater salinity proxy record from a subtropical gyre deep-sea sediment core. We show that North Atlantic gyre surface salinities oscillated rapidly between saltier stadial conditions and fresher interstadials, covarying with inferred shifts in the Tropical Atlantic hydrologic cycle[6] and North Atlantic overturning circulation. These salinity oscillations suggest a reduction in precipitation into the North Atlantic and/or reduced export of deep salty thermohaline waters during stadials. We hypothesize that increased stadial salinities preconditioned the North Atlantic Ocean for a rapid return to deep overturning circulation and high-latitude warming by contributing to increased North Atlantic surface-water density on interstadial transitions.

Through its influence on regional evaporation–precipitation patterns in the North Atlantic basin[3,7,8], atmospheric freshwater transport plays an important part in maintaining the increased North Atlantic gyre surface salinities that promote meridional overturning circulation (MOC). Net evaporation exceeds precipitation in the western subtropical North Atlantic gyre, increasing the surface salinity of the Gulf Stream as it circulates northward through the subtropics[3,9]. After these surface waters reach subpolar latitudes and warm the atmosphere, the excess salt is critical in maintaining modern North Atlantic MOC (ref. 10). It is generally agreed that rapid climate shifts associated with Dansgaard–Oeschger cycles during the last glacial period were triggered by changes in surface water density at the sites of deep water formation in the North Atlantic[2,4,5]. Whereas warm interstadials were characterized by a circulation pattern similar to that of the present, the northward flow of warm, salty surface waters into the subpolar North Atlantic was reduced and/or subducted below a cold, fresh surface layer during stadials[4,5]. As a result, stadial surface temperatures plummeted in the northern North Atlantic region and the sites of deep-water formation migrated south of the stadial polar front (Fig. 1).

We reconstruct surface salinities (as seawater $\delta^{18}O$, $\delta^{18}O_{SW}$) across four Dansgaard–Oeschger cycles at Ocean Drilling Program (ODP) site 1060 located on the Blake Outer Ridge near the modern position of the northward flowing Gulf Stream (Fig. 1). Seawater $\delta^{18}O$ covaries linearly with surface salinity, making it one of the most direct proxies for estimating salinity in the modern ocean[11]. Because foraminiferal calcite ($\delta^{18}O_C$) is controlled by temperature and $\delta^{18}O_{SW}$, $\delta^{18}O_{SW}$ can be computed if temperature is determined independently. Using combined Mg/Ca palaeothermometry and $\delta^{18}O$ analyses of shells from the surface-dwelling foraminifera *Globigerinoides ruber* (white variety), we produce a continuous millennial-scale record (4 cm sampling, 75–250-year resolution) of gyre $\delta^{18}O_{SW}$ variability. We use previously published methods[12,13] for measurements and for calculations of $\delta^{18}O_{SW}$. Our results are presented on a previously published age model developed for site 1060 based on correlations between the percentage of warm surface-dwelling planktonic foraminifera and changes in atmospheric temperature over Greenland as determined from the Greenland Icecore Project (GRIP) ice $\delta^{18}O$ record[14] (see Supplementary Figs 1 and 2).

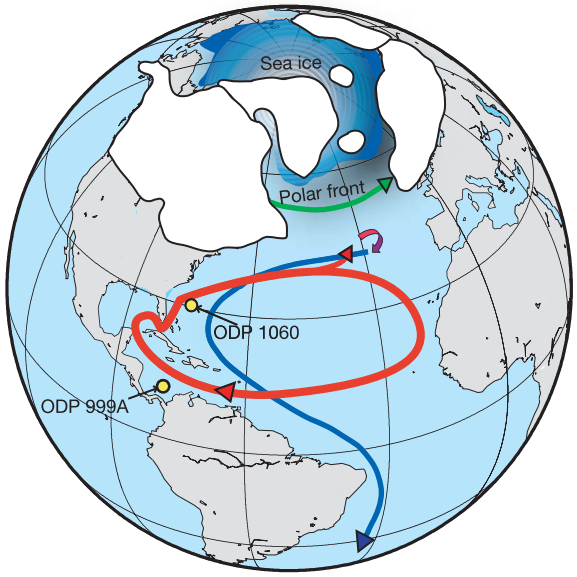

Figure 1 | Idealized North Atlantic surface (red arrows) and deep water (blue arrow) circulation during MIS 3 stadial events. Flow paths are based on modern patterns. The locations of ODP site 1060 (30° 46′ N, 74° 28′ W; 3,480 m; 20–53 cm kyr^{-1} sedimentation rate) and ODP site 999A (12° 45′ N, 78° 44′ W) are indicated. The stadial mode of overturning circulation results from the convection of surface waters south of the polar front. The extent of continental ice sheets is estimated from ref. 30.

[1]Department of Geology, University of California, Davis, California 95616, USA. [2]Godwin Laboratory for Palaeoclimate Research, University of Cambridge, Cambridge CB2 3EQ, UK. †Present addresses: School of Earth and Atmospheric Sciences, Georgia Institute of Technology, Atlanta, Georgia 30332, USA (M.W.S.); British Antarctic Survey, High Cross, Madingley Road, Cambridge CB3 0ET, UK (M.J.V.).

The *G. ruber* $\delta^{18}O_C$ record from site 1060 displays clear isotopic oscillations with the lowest values occurring during warm interstadial events and the highest values occurring during cold stadials (Fig. 2a). Average stadial–interstadial amplitudes are ~0.7‰. Interstadial $\delta^{18}O_C$ values are lowest during the middle of interstadials and gradually increase during the latter part of warm phases.

Mg/Ca ratios in *G. ruber* were converted to sea surface temperature (SST) using a species-specific, depth-corrected relationship calibrated for the Atlantic[15]. Mg/Ca SSTs from site 1060 (Fig. 2b) do not mirror the GRIP ice $\delta^{18}O$ record (Fig. 2e). Whereas the transitions into interstadials 12, 13, 15, and 16 show a SST increase, temperature change at the transition into interstadial 14 is indistinct. Although Mg/Ca SSTs during the latter part of interstadials 14 and 16 are similar to or lower than faunal-based August SST calculations[14], Mg/Ca SSTs are warmer than August faunal temperatures during the remaining interstadials and are as much as 5 °C warmer than August faunal SSTs during stadials (Fig. 2b). Mg/Ca and Sr/Ca ratios in *G. ruber* shell material from site 1060 do not covary and Mg/Ca ratios do not correlate with a nearby benthic *Cibicidoides wuellerstorfi* $\delta^{13}C$ record also on the Blake Outer Ridge, suggesting that dissolution and stadial–interstadial changes in bottom-water masses at site 1060 have not affected our reconstructed SST record (see Supplementary Information Figs 3 and 4).

Because foraminiferal productivity is seasonally biased, *G. ruber* and other species will not record annual mean SST[16,17]. The observation that Mg/Ca SST reconstructions are similar to August faunal SST estimates at site 1060 during interstadials (Fig. 2b) suggests that *G. ruber* inhabited the water column above site 1060 during the warmest summer months of marine isotope stage (MIS) 3. In addition, the largest temperature differences between the faunal and the Mg/Ca SST reconstructions occur during stadials. One possible explanation for the offset between proxies is that a steep stadial temperature gradient existed in this region of the subtropical gyre. As a result, *G. ruber* would have been excluded from the faunal population above site 1060 during most of the year when the frontal boundary was located south of site 1060. However, when northward movement of the meandering Gulf Stream shifted the frontal boundary near site 1060 during the warmest years and summer months, subtropical gyre waters containing *G. ruber* would have provided a source for the flux of this species to the sediment. We therefore interpret the *G. ruber* geochemical record to reflect late summer conditions in the subtropical gyre. Most important for salinity reconstructions is the fact that $\delta^{18}O_C$ and Mg/Ca SST are measured on material from the same population of *G. ruber*. Hence, these two geochemical proxies are linked to the same physical properties of the surface ocean, thereby allowing us to compute and compare $\delta^{18}O_{SW}$ values at site 1060 when *G. ruber* was present.

Removing temperature from the $\delta^{18}O_C$ record using the temperature–$\delta^{18}O$ relationship that has been field-calibrated for use with white *G. ruber* (ref. 18) yields the salinity proxy $\delta^{18}O_{SW}$ (Fig. 2c). Unlike Mg/Ca SST, $\delta^{18}O_{SW}$ values at site 1060 show clear salinity shifts that relate to stadial–interstadial phases in the GRIP $\delta^{18}O$ ice record[1] (Fig. 2e). However, bioturbation and potential age model errors do not allow us to determine definitively the timing of these $\delta^{18}O_{SW}$ transitions relative to changes in the GRIP ice core. Nevertheless, stadial events are characterized by the abrupt development of saltier, more positive $\delta^{18}O_{SW}$ values that average between 2.2 and 2.3‰. In contrast, interstadials 16, 14, and 12 have $\delta^{18}O_{SW}$ values that average between 1.7 and 1.9‰. The previously reconstructed MIS 3 $\delta^{18}O_{SW}$ values in the Caribbean core ODP 999A are consistent with the average stadial–interstadial site 1060 $\delta^{18}O_{SW}$ values from 45 to 60 kyr (ref. 13) (see Supplementary Fig. 5).

Although the magnitude of sea level change during MIS 3 has yet to be determined precisely, changes in sea level cannot account for the 0.3–0.6‰ $\delta^{18}O_{SW}$ differences between stadial–interstadial phases (see Supplementary Fig. 6). We therefore conclude that the majority of the $\delta^{18}O_C$ variation seen in *G. ruber* is due to salinity change, and consider these $\delta^{18}O_{SW}$ shifts a robust reflection of Gulf Stream/gyre surface salinity variability during MIS 3. If we assume that the $\delta^{18}O_{SW}$–surface salinity relationship for the southwestern North Atlantic gyre during MIS 3 was similar to the modern relationship[19],

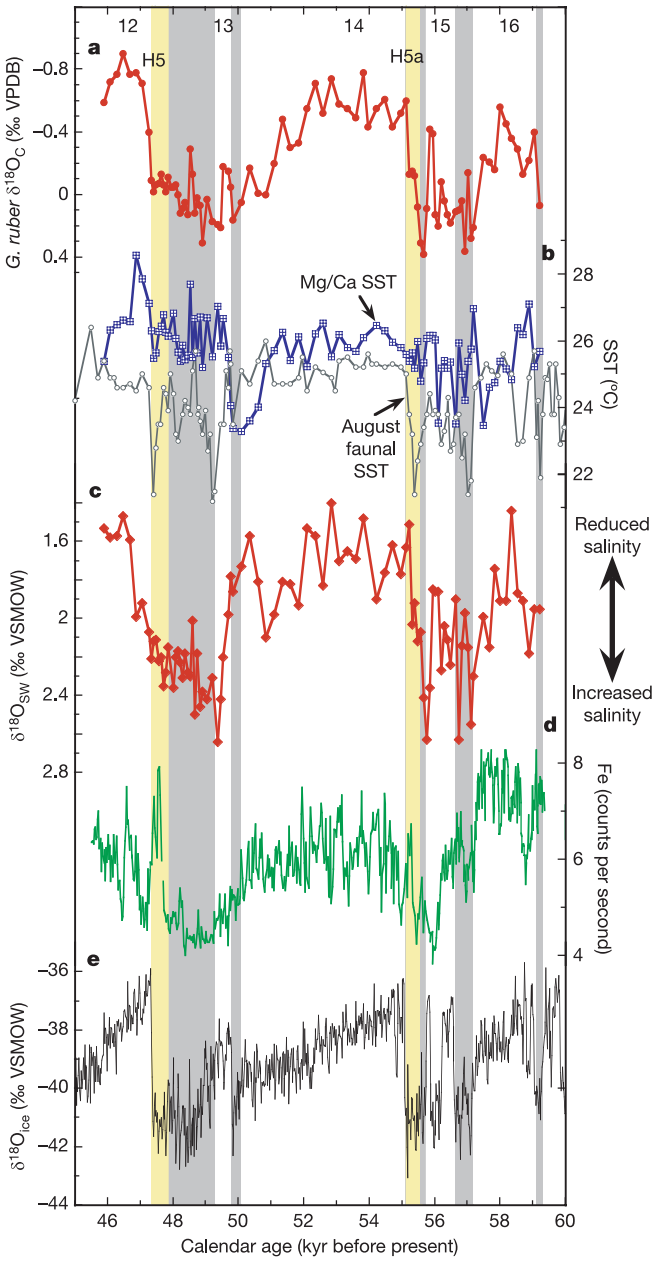

Figure 2 | Temperature and salinity variation at site 1060 during MIS 3. **a**, *G. ruber* (white variety) $\delta^{18}O_C$ from site 1060 (solid red circles). VPDB, Vienna Pee-Dee belemnite standard. **b**, Mg/Ca SSTs (blue crossed squares) from site 1060. Mg/Ca ratios were converted to SST using[15] $Mg/Ca = 0.38 \times e^{0.09(SST-0.61d)}$, where SST is in °C and *d* is the depth of the core in kilometres. The faunal SST reconstructions for August (grey open circles) calculated from the foraminiferal assemblages[14] are also shown for comparison. **c**, Computed $\delta^{18}O_{SW}$ from site 1060 (solid red diamonds) calculated from the Mg/Ca-derived SST and $\delta^{18}O_C$ using T (in °C) = 16.5–4.80($\delta^{18}O_C - (\delta^{18}O_{SW} - 0.27‰)$). **d**, Fe content (counts per second) from the Cariaco basin core ODP site 1002 (ref. 6), adjusted to the GRIP age model. **e**, GRIP $\delta^{18}O_{ICE}$ record[1]. Cold stadials in the GRIP record are marked by more arid conditions in the western tropical Atlantic (lower Fe concentrations) and elevated gyre salinities (increased $\delta^{18}O_{SW}$ values at site 1060). Note the salinity increases (as $\delta^{18}O_{SW}$) associated with the shaded stadial events and the reduced salinities associated with interstadials. Numbered interstadials 12 to 16 and Heinrich events H5 and H5a (yellow bars) are labelled at the top of the figure.

$\delta^{18}O_{SW} = 0.4 \times$ (surface salinity)–13.5, then average stadial–interstadial $\delta^{18}O_{SW}$ values suggest millennial-scale surface-salinity enrichments of 0.7 to 1.5 during stadials (see 'Error analysis' in Methods).

Changes in the Fe and Ti content in the Cariaco basin core ODP 1002 (ref. 6) provides a high-resolution record of high to low latitude air–sea linkages in the Atlantic during MIS 3. These data suggested that the intertropical convergence zone (ITCZ) migrated southward during cold stadial events in the North Atlantic, resulting in reduced freshwater precipitation over northeastern South America and reduced river-borne delivery of Fe and Ti to the Cariaco basin[6]. Although our site 1060 $\delta^{18}O_{SW}$ record is of lower resolution, wet/dry periods in the ODP site 1002 Fe record covary with changes in surface $\delta^{18}O_{SW}$ values at site 1060 (Fig. 2c and d). Wet interstadials 16, 14 and 12 correspond to periods of reduced $\delta^{18}O_{SW}$ values at site 1060. Likewise, the sustained period of arid conditions in the Cariaco basin after interstadial 14 (49.2–47.7 kyr) corresponds to enriched $\delta^{18}O_{SW}$ values in the gyre. Neither the Cariaco basin Fe record nor the site 1060 $\delta^{18}O_{SW}$ record show the predicted response to the interstadial 13 warming recorded in the GRIP ice core (Fig. 2).

During periods of high-latitude cooling, general circulation model (GCM) simulations predict increased northeast trade wind strength associated with an intensification of the subtropical high pressure located over the southwestern North Atlantic gyre[20,21]. These conditions result in a precipitation deficit in the tropical and subtropical North Atlantic coupled with a freshening of the tropical and subtropical South Atlantic. Speleothem records from Brazil indicate that the South Atlantic experienced enhanced freshwater input during cool stadial events in the north[22], just as our $\delta^{18}O_{SW}$ reconstruction from site 1060 indicates elevated salinities in the North Atlantic gyre. This dipole wet/dry relationship between the North and South Atlantic implies that the tropical hydrologic cycle helps to regulate the meridional salinity gradient in the Atlantic basin.

GCM modelling of North Atlantic MOC stability under glacial boundary conditions also suggests that the tropical Atlantic hydrologic cycle shifts to an enhanced evaporative regime, resulting in glacial North Atlantic MOC stabilization[23,24]. The increased stadial gyre salinities that we record at site 1060 are therefore consonant with the stable mode of haline-driven glacial North Atlantic MOC found in these models[23,24]. We hypothesize that the stadial mode of MOC, coupled with a southward shift of the ITCZ, resulted in reduced oceanic salt export and reduced tropical precipitation into the north Atlantic. Together, these led to the rapid accumulation of salt in the North Atlantic subtropical gyre on transitions into stadials. Then, as the low-salinity surface waters and sea ice retreated in the high-latitude North Atlantic on interstadial transitions[5], the positive gyre salinity anomalies would have penetrated northward within the North Atlantic Drift, elevating surface water density in the Greenland–Iceland–Norwegian seas and the Labrador Sea and promoting the resumption of vigorous interstadial MOC.

Reconstruction of $\delta^{18}O_{SW}$ from the western equatorial Pacific also indicates elevated stadial surface salinities (ref. 25), suggesting a link between North Atlantic stadials and El Niño-like conditions in the tropical Pacific. Coupled GCM[26,27] and reanalysis results[28] show that El Niño conditions also result in enhanced water vapour removal from the tropical Atlantic. In addition, historical data indicate that the mean position of the ITCZ is displaced southward during an El Niño phase, resulting in a rainfall deficit in Central America[29]. If the freshwater perturbations associated with El Niño conditions persisted for longer periods (such as during MIS 3 stadials), this could reinforce the drying effects of a more southerly ITCZ and contribute to the elevated stadial salinities we record in the North Atlantic gyre at site 1060.

Stadial–interstadial reorganizations of the tropical Atlantic hydrologic cycle therefore had a significant impact on the freshwater balance of the North Atlantic subtropical gyre. As the ITCZ migrated southward during stadials, enhanced water vapour removal from the North Atlantic led to the development of positive salinity anomalies in the subtropical gyre, contradicting the hypothesis that interstadials are periods of increased freshwater export from the Atlantic[6]. A shift to enhanced El-Niño-like stadial circulation in the eastern tropical Pacific may also have contributed to increased tropical Atlantic aridity. If, as we predict, increased surface salinities in the western subtropical gyre are indicative of an overall enrichment in the North Atlantic gyre's mixed-layer salinity during stadials, then the tropical hydrologic cycle acts as a negative feedback during weak phases of MOC, increasing North Atlantic surface water density and preconditioning the system for a return to an interstadial mode of strong MOC.

METHODS

Sample preparation. Sediment samples were collected from site 1060 at 4 cm resolution. Each core interval was disaggregated in ultrapure water, sieved and dried at room temperature. If possible, specimens of *G. ruber* (white variety) were then collected from the 250–350-μm size fraction and 25 shells were combined for each stable isotope analysis for downcore measurements to minimize intraspecific variation in shell geochemistry. These samples were sonicated in methanol for 5–10 s, roasted in vacuum at 375 °C for 30 min, and analysed on a Fisons Optima infrared mass spectrometer using an Isocarb common acid bath autocarbonate system at 90 °C at the University of California, Davis. During stadial intervals, *G. ruber* abundance was much lower, so it was necessary to collect all specimens >63 μm in size in certain intervals. In these intervals, all available specimens were pooled and gently crushed. A separate split of the homogenized sample (approximately 40 μg) was roasted and analysed for stable isotopes and the remainder of the shell material was analysed for trace and minor elements.

Elemental ratio measurement. Mg/Ca ratios were measured on foraminifera collected from the same population and size fraction that was used for the stable isotope analyses. Where possible, approximately 600 μg of material per sample (~55 shells) was cleaned for trace- and minor-element analysis without a DTPA step[12]. Briefly, samples underwent a multi-step process consisting of initial rinses in ultrapure water, followed by treatments with hot reducing and oxidizing solutions, transfers into new acid-leached micro-centrifuge vials, and finally leaches with a dilute ultrapure acid solution. All sample cleaning was conducted in laminar flow benches under trace-metal-clean conditions. Samples were then dissolved and analysed on a Finnigan Element-2 inductively coupled plasma mass spectrometer at the University of California, Santa Barbara, using established procedures[12].

Elemental ratios of Fe/Ca and Al/Ca were used to monitor cleaning efficacy. Fe/Ca ratios remain $<130\ \mu mol\ mol^{-1}$ and Al/Ca ratios remain $<50\ \mu mol\ mol^{-1}$ throughout the record, indicating that Mg contamination associated with detrital sediment in cleaned samples was not a problem[17]. Although Mg/Ca does show a statistically significant correlation with Fe/Ca, levels of Fe are three orders of magnitude smaller than Mg in the cleaned samples, so Fe-bearing minerals not removed during the cleaning process cannot contribute significantly to the primary Mg/Ca signal in the foraminiferal calcite.

Error analysis. Analytical precision for the $\delta^{18}O_C$ measurements is better than ±0.06‰. The pooled standard deviation of replicate Mg/Ca analyses from site 1060 was ±2.9% (1 standard deviation (s.d.); degrees of freedom = 49; 51% of the intervals run in replicate). The s.d. for the $\delta^{18}O_{SW}$ residual was calculated to be ±0.2‰ (1 s.d.) using a Monte Carlo methodology that assumed a normal distribution in the $\delta^{18}O_C$ and Mg/Ca errors and in the Mg/Ca-SST and $\delta^{18}O_C$-SST calibration precision.

The conversion of the $\delta^{18}O_{SW}$ proxy to salinity is difficult to constrain owing to uncertainties in the slope of the relationship between these two variables at times in the past. However, it is likely that the slope of this relationship was steeper during glacial times owing to the input of isotopically depleted fresh water, reducing the millennial-scale surface salinities change in the gyre to <1 salinity unit.

Received 19 December 2005; accepted 27 July 2006.

1. Johnsen, S. J. *et al.* Oxygen isotope and palaeotemperature records from six Greenland ice-core stations: Camp Century, Dye-3, GRIP, GISP2, Renland and NorthGRIP. *J. Quat. Sci.* **16,** 299–307 (2001).
2. Boyle, E. A. Is ocean thermohaline circulation linked to abrupt stadial/interstadial transitions? *Quat. Sci. Rev.* **19,** 255–272 (2000).
3. Broecker, W. S., Bond, G., Klas, M., Bonani, G. & Wolfli, W. A salt oscillator in the glacial Atlantic? The concept. *Paleoceanography* **5,** 469–478 (1990).

4. Oppo, D. W. & Lehman, S. J. Suborbital timescale variability of North Atlantic deep water during the past 200,000 years. *Paleoceanography* **10,** 900–910 (1995).
5. Rasmussen, T. & Thomsen, E. The role of the North Atlantic Drift in the millennial timescale glacial climage fluctuations. *Palaeogeogr. Palaeoclim. Palaeoceanogr.* **210,** 101–116 (2004).
6. Peterson, L. C., Haug, G. H., Hughen, K. A. & Rohl, U. Rapid changes in the hydrologic cycle of the Tropical Atlantic during the last Glacial. *Science* **290,** 1947–1951 (2000).
7. Broecker, W. S. The salinity contrast between the Atlantic and Pacific during glacial time. *Paleoceanography* **4,** 207–212 (1989).
8. Zaucker, F. & Broecker, W. S. The influence of atmospheric moisture transport on the fresh water balance of the Atlantic drainage basin: general circulation model simulations and observations. *J. Geophys. Res.* **97,** 2765–2773 (1992).
9. Curry, R., Dickson, B. & Yashayaev, I. A change in the freshwater balance of the Atlantic Ocean over the past four decades. *Nature* **426,** 826–829 (2003).
10. Broecker, W. S. The great ocean conveyor. *Oceanography* **4,** 79–89 (1991).
11. Craig, H. & Gordon, L. I. in *Stable Isotopes in Oceanographic Studies and Paleotemperatures* (ed. Tongiorgi, E.) 9–130 (CNR, Pisa, 1965).
12. Lea, D. W., Pak, D. K. & Spero, H. J. Climate impact of Late Quaternary equatorial Pacific sea surface temperature variations. *Science* **289,** 1719–1724 (2000).
13. Schmidt, M. W., Spero, H. J. & Lea, D. W. Links between salinity variation in the Caribbean and North Atlantic thermohaline circulation. *Nature* **428,** 160–163 (2004).
14. Vautravers, M. J., Shackleton, N. J., Lopez-Martinez, C. & Grimalt, J. O. Gulf Stream variability during marine isotope stage 3. *Paleoceanography* **19,** PA2011, doi:10.1029/2003PA000966 (2004).
15. Dekens, P. S., Lea, D. W., Pak, D. K. & Spero, H. J. Core top calibration of Mg/Ca in tropical foraminifera: refining palaeotemperature estimation. *Geochem. Geophys. Geosyst.* **4,** doi:10.1029/2001GC000200 (2002).
16. Deuser, W. G., Ross, E. H., Hemleben, C. & Spindler, M. Seasonal changes in species composition, numbers, mass, size, and isotopic composition of planktonic-foraminifera settling into the deep Sargasso Sea. *Palaeogeogr. Palaeoclimatol. Palaeoecol.* **33,** 103–127 (1981).
17. Schmidt, M. W., Vautravers, M. J. & Spero, H. J. Western Caribbean sea surface temperatures during the Late Quaternary. *Geochem. Geophys. Geosyst.* **7**, doi:10.1029/2005GC000957 (2006).
18. Thunell, R., Tappa, E., Pride, C. & Kincaid, E. Sea-surface temperature anomalies associated with the 1997–1998 El Nino recorded in the oxygen isotope composition of planktonic foraminifera. *Geology* **27,** 843–846 (1999).
19. Schmidt, G. A., Bigg, G. R. & Rohling, E. J. *Global Seawater Oxygen-18 Database* ⟨http://data.giss.nasa.gov/o18data/⟩ (1999).
20. Lohmann, G. Atmospheric and oceanic freshwater transport during weak Atlantic overturning circulation. *Tellus A* **55,** 438–449 (2003).
21. Vellinga, M. & Wu, P. L. Low-latitude freshwater influence on centennial variability of the Atlantic thermohaline circulation. *J. Clim.* **17,** 4498–4511 (2004).
22. Wang, X. F. *et al.* Wet periods in northeastern Brazil over the past 210 kyr linked to distant climate anomalies. *Nature* **432,** 740–743 (2004).
23. Prange, M., Romanova, V. & Lohmann, G. The glacial thermohaline circulation: stable or unstable? *Geophys. Res. Lett.* **29**, doi:10.1029/2002GL015337 (2002).
24. Romanova, V., Prange, M. & Lohmann, G. Stability of the glacial thermohaline circulation and its dependence on the background hydrological cycle. *Clim. Dyn.* **22,** 527–538 (2004).
25. Stott, L. D., Poulsen, C., Lund, S. & Thunell, R. Super ENSO and global climate oscillations at millennial time scales. *Science* **297,** 222–226 (2002).
26. Latif, M., Roeckner, E., Mikolajewicz, U. & Voss, R. Tropical stabilization of the thermohaline circulation in a greenhouse warming simulation. *J. Clim.* **13,** 1809–1813 (2000).
27. Schmittner, A. & Clement, A. C. Sensitivity of the thermohaline circulation to tropical and high latitude freshwater forcing during the last glacial–interglacial cycle. *Paleoceanography* **17**, doi:10.1029/2000PA (2002).
28. Schmittner, A., Appenzeller, C. & Stocker, T. F. Enhanced Atlantic freshwater export during El Nino. *Geophys. Res. Lett.* **27,** 1163–1166 (2000).
29. Hastenrath, S. The intertropical convergence zone of the eastern Pacific revisited. *Int. J. Climatol.* **22,** 347–356 (2002).
30. Peltier, W. R. Ice Age paleotopography. *Science* **265,** 195–201 (1994).

Supplementary Information is linked to the online version of the paper at www.nature.com/nature.

Acknowledgements We thank the Ocean Drilling Program for core samples. Funding for this research was provided by JOI-ODP Schlanger Ocean Drilling Fellowships to M.W.S. and by a US National Science Foundation grant to H.J.S. Laboratory assistance from D. Pak and mass spectrometer operation by G. Paradis and D. Winter were critical to the success of this study. Elemental analyses were conducted in D. Lea's laboratory at the University of California, Santa Barbara. We also thank A. Russell and D. Lea for discussions and comments.

Author Information Reprints and permissions information is available at www.nature.com/reprints. The authors declare no competing financial interests. Correspondence and requests for materials should be addressed to M.W.S. (mschmidt@eas.gatech.edu).